

---

# High accuracy polarimetry and its application

Y.Shopa

Ivan Franko L'viv National University, 8 Kyryl and Mefodiy Street, L'viv, 79005, Ukraine

Received 05.06.2001

## Abstract

The principles of high accuracy polarimetry are described. The methods of simultaneous measurements of birefringence and optical activity in anisotropic directions of crystals are considered. The measurement technique and experimental results of first polarization methods on the base of the azimuthal oscillations and high accuracy null polarimetry, HAUP, tilter system are analyzed. The attention is paid to a method that is similar to HAUP, which was designed with participation of the author and is used for studying of a number of crystals.

**Keywords:** Optical activity, birefringence, polarimetry, HAUP

**PACS:** 78.20.Ek; 78.20.Fm; 95.75.Hi

<b>Introduction</b>	<b>58</b>
<b>1. Eigen wave in gyrotropic crystals</b>	<b>59</b>
<b>2. Early polarization methods</b>	<b>60</b>
<b>3. High-accuracy universal polarimeter</b>	<b>62</b>
<b>4. Azimuthal rotation measurements</b>	<b>64</b>
<b>5. High accuracy PSCA null polarimeter</b>	<b>66</b>
<b>6. Polarimetric method related to HAUP</b>	<b>67</b>
<b>6.1. Experiments with optically nonactive samples</b>	<b>69</b>
<b>6.2. Sample rotation by 90°</b>	<b>70</b>
<b>7 Tilter polarimeter</b>	<b>71</b>
<b>Conclusion</b>	<b>73</b>
<b>References</b>	<b>74</b>

## Introduction

Polarimetry is one of the most sensitive method of studying of the origins of phase transitions of solids, including incommensurate transitions; the analysis of the structural units configuration of solids, including chiral high polymers; and the accurate determination of symmetry elements and twinning of crystals [1–3].

The founding of the new phenomena in physical optics – electrogyration [4] makes a strong pulse in the development of precise

methods of measuring of optical activity. Being an electrical analogue of Faraday effect, which is known from the middle of the XIX centuries [5], the electrogyration unfortunately is not mentioned in the known textbooks. At the same time magnetic analog of the Pockels effect called Cotton-Mouton effect is featured in each physical textbook for higher school. Perhaps it is connected with the fact that the electrogyration (Vlokh–Zheludev phenomenon) is a quite small effect in known media and have not

found yet the applications in optoelectronics. But from the fundamental point of view the founding of this effect is very important for the understanding of the nonlinear electrodynamic.

Number of objects, in which the electrogyration was measured by induced rotation of the linear polarization of the light along optical axis is rather insignificant [4]. On the cover page of this journal the so-called interference conoscopic pictures, are presented which are obtained with Li-doped lead germanate crystals. The electrical voltage of the value 5 kV, applied to a crystal at temperatures 430 K leads to the noticeable light transmittance in the center of the crossed isogyres. Probably it is an unusual case of the visual observation of electrogyration.

In most cases optical activity and electrogyration can be observed at the conditions of the presence of linear birefringence. The measuring of the optical activity in the birefringent sections is difficult because the linear birefringence is typically 1000×larger than either of the circular effects [6]. The methods of their measuring in such conditions are more complicated, but the obtained results are usually quite interesting.

During last years the interest to polarimetry remains significant. A number of scientific centers take part in the development of the theory and practice of such measuring [5,7–11]. The present review is devoted to the technical aspects of polarimetric measurements by high-accuracy polarimetry as well as a detail studying of optical rotation and electrogyration. The principle problem in the high-accuracy universal polarimeter is removing the characteristic parasitic errors in a linearly birefringent and optically active crystal. The supersensible polarization measuring which is also interesting is out of the text of this paper.

## 1. Eigen wave in gyrotropic crystals

Propagation of the electromagnetic waves through the crystals can be characterized by so-called eigen waves [4,6,12]. If a linearly polarized

light beam incident normally to a crystal plate in general case it splits into two elliptically polarized waves, that propagate in the crystal with different refractive indices  $n_1$  and  $n_2$ , eigen waves ellipticities  $k_1$ ,  $k_2$  and non-orthogonal polarization ellipses. In transparent crystals the eigen waves are orthogonal and  $k_1 = -k_2 = k$ . The total phase difference  $\Delta$  between the two eigen waves is calculated as

$$\Delta = \frac{2\pi}{\lambda} \left[ (n' - n'')^2 + \frac{G^2}{n'n''} \right]^{1/2}, \quad (1)$$

where  $G$  is the scalar parameter of gyration (usually called 'gyration'),  $n'$  and  $n''$  are refractive indices of the nongyrotropic crystal. Gyration  $G$  depends on the gyration tensors components  $g_{ij}$  and on the wave normal direction cosines  $l_i, l_j$  [12]

$$G = g_{ij} l_i l_j. \quad (2)$$

On the other hand

$$\Delta^2 = \delta^2 + (2\rho)^2, \quad (3)$$

where  $\delta = (2\pi/\lambda)(n' - n'')$  is the partial phase difference and  $\rho = \pi G/\lambda \bar{n}$  is the specific optical rotation,  $\bar{n} = \sqrt{n'n''}$  is the mean refractive index. The ellipticity  $k$  is the same for the both elliptically polarized waves in the crystal and is given as

$$k = \frac{1}{2} \arctan \left( \frac{2\rho}{\delta} \right). \quad (4)$$

All methods for measuring the optical activity in birefringent directions are based on the obtaining of the ellipticity of the eigen (= normal) waves,  $k$ , from the polarization state of the beam emerged from the crystal. Scalar parameter of gyration  $G$  is calculated simply as

$$G = 2k(n' - n'')\bar{n}. \quad (5)$$

The electrogyration effect is due to the change of the gyration  $G$  under the influence of the electric field. Its detailed definition can be found in the book [4].

## 2. Early polarization methods

The first reliable result of a gyrotropy measurement in a birefringent direction was obtained by Szivessy and Münster in quartz [13] on the basis of the emergent beam analysis using null-photometry method. They have determined three special input azimuth  $\theta$  (Fig. 1), polarization state which can be easily identified by null-polarimetry method. It was offered also to vary experimental conditions (change phases difference and crystal orientation) for the determination of the  $k$ . Factually these Szivessy and Münster's ideas were used in all next methods.

Except Bruhat and Grivet investigations [14], that essentially improved measuring technique, no body has been conducting similar

studying for a long time. Interest to them returned only after the investigations of Konstantinova et al [15] who obtained the relations of the ellipticity and azimuth of deviation of ellipse of the polarization of waves passed through the anisotropic gyrotropic crystals. Besides the extension of the investigations was stimulated by the possibility of the existing of the electrogyration – effect that was predicted by Zheludev in 1964 [16]. The experimental confirmation of this effect was made only in 1969 by O.Vlokh [17].

Ellipticity of the light that emerges the sample (scheme on Fig. 1) in the case of small  $\theta$  also is small. The relations for  $\chi$ -angle and ellipticity  $\varepsilon$  can be written as:

$$\tan 2\chi = \frac{\tan 2\theta \cos \Delta - \frac{2k}{1+k^2} \sin \Delta}{\frac{1-k^2}{1+k^2} + \left(\frac{2k}{1+k^2}\right)^2 \cos \Delta + \frac{2k}{1+k^2} \tan \theta \sin \Delta}, \quad (6)$$

$$\sin 2\varepsilon = \frac{1-k^2}{1+k^2} \left[ \sin 2\theta \sin \Delta + \frac{2k}{1+k^2} \cos 2\theta (1 - \cos \Delta) \right], \quad (7)$$

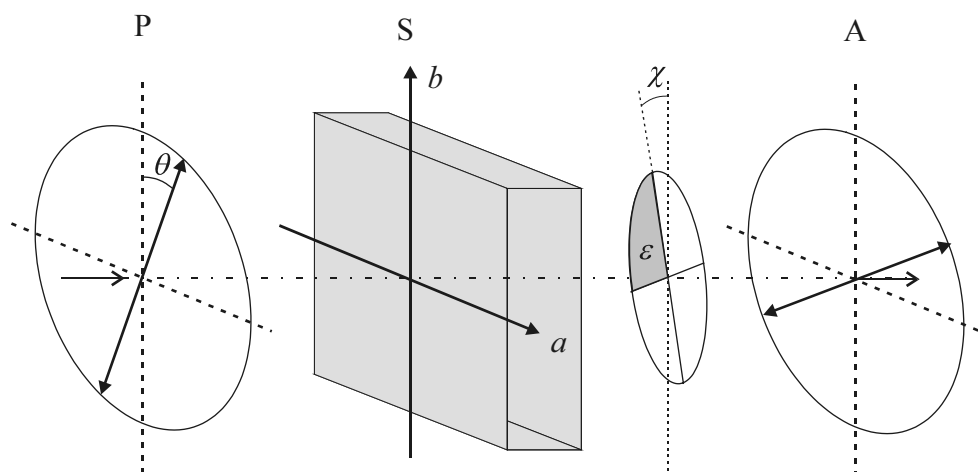


Fig.1 Relation between the polarization azimuth  $\theta$  of the incident wave of the linearly polarized light,  $a$  and  $c$  crystallophysical axes of the crystal and azimuth  $\chi$  of emergent light with the ellipticity  $\varepsilon$  in classic polarizer–sample–analyzer (PSA) polarimeter.

One of the ways of the investigating of optical activity and determination of the gyration tensor component is to use the relationships (6) with neglecting of the terms with  $k^2$  and on conditions of providing  $\theta = 0$

$$\tan 2\chi = -2k \sin \Delta, \quad \sin 2\varepsilon = 2k(1 - \cos \Delta). \quad (8)$$

To measure the passed light azimuth it is necessary to set the investigated plate in the extinction position between crossed polarizers. Then, by changing  $\Delta$ , e.g. the wavelength of the incident light or temperature, one can measure the change of the passed light azimuth polarization  $\chi$ . Fig. 2 gives the values of the very known dependence of angle  $\chi$  on  $\lambda$  for quartz crystals ( $\text{SiO}_2$ ) cut out parallel to the optical axis [15]. Authors noticed the difference in oscillations amplitude  $\chi_{\parallel}$  and  $\chi_{\perp}$  at the rotation of the crystal at  $90^\circ$  around optical beam. This difference is connected with additional ellipticity, which is impossible to eliminate. However in other experiments that were conducted by Vlokh et al [18] such a difference was not observed. In this paper it was particularly shown, that  $\frac{\tan 2\chi_{\parallel}}{\tan 2\chi_{\perp}} = \frac{n'}{n''}$ , and it is practically impossible to detect such a small difference [18,19].

The method proposed by Konstantinova has been widely used, particularly by Ivanov and Konstantinova [20], Ivanov and Chikhladze [21], Kaminskii et al [22], Vlokh et al [23,24]. First measurements of the electrogyration in anisotropic directions of crystals are conducted by Vlokh [25]. For most crystals this method gives quite satisfactory results. From other side the azimuthal measurements in crystals with a so-called isotropic point are rather interesting [4]. For the first time photometrical method of the measuring optical activity was implemented by Anderson et al for  $\text{AgGeS}_2$  crystals [26]. These crystals were also actively studied by Vlokh and Zaryk within the method of oscillations of azimuth of polarization [24].

In the case of small ellipticity of normal waves ( $k < 0.001$ ), the measuring errors of optical activity increase, and the induced effects, such as electrogyration, become undetected for apparatus. In such requirements the magnitude of experimental errors will essentially increase. Even if to take into account the probable parasitic ellipticity one can not obtain good results.

The usage of constant systematic errors typical for each particular polarimetric system is shown to be inappropriate [4,7,27]. These errors

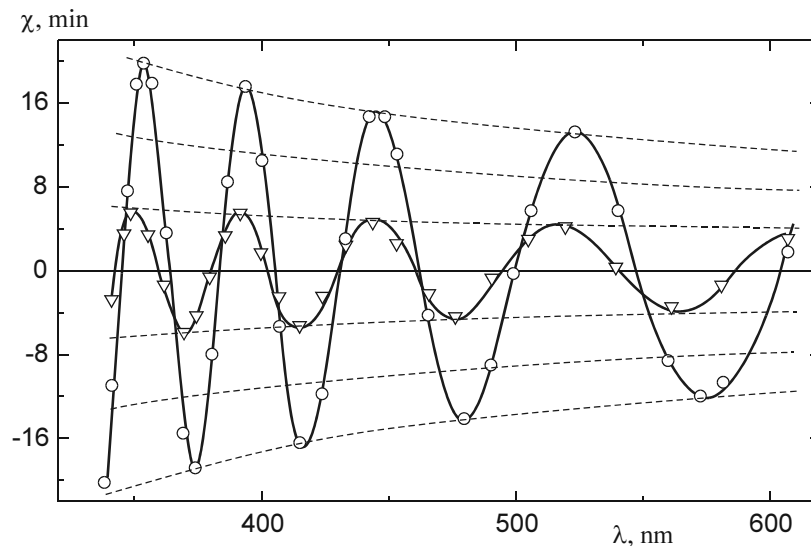


Fig.2 Dependence of the passed light azimuth of the polarization  $\chi$  on the wavelength  $\lambda$  for quartz crystals [15]. The difference between two crystals positions (O,  $\nabla$ ) turned by  $90^\circ$  around optical beam is visible.

should preferably be determined in each measurement process, since the instrumental parasitics depend not only on the optical and mechanical elements of the experimental system (polarizers, rotators, detection unit etc.), but on sample quality, alignment of the system, and even in many cases exactly where the light beam passes through the sample. Thus, measurements with different samples give different values of parasitic errors.

Probably just such errors have been observed by Konstantinova et al [15] (Fig. 2). Instrumental parasitics can be held within the same order of the magnitude for different samples ( $10^{-4}$ ) if they are of good optical quality. However, the parasitics are increased by an order of magnitude the ( $10^{-3}$ ) if the samples are of bad optical quality [7]. Such problems have required new solutions in a polarimetry. They were found by Kobayashi [27,28] and are tested on the quartz crystals [29].

### 3. High-accuracy universal polarimeter

Invented by Kobayashi, high-accuracy universal polarimeter (HAUP) facilitates the simultaneous measurement of optical activity, birefringence and rotating angles of indicatrix of crystals. HAUP eliminates many of the difficulties associated with the separation of optical activity of low symmetry crystals from the linear birefringence, and ensures more accurate measurement of birefringence of the crystals belonging to monoclinic and triclinic systems, since indicatrices of these crystals rotate by the changing of the temperature, wavelengths, etc. [3].

HAUP is composed of simple optical elements polarizer–sample–analyzer (PSA). Before setting the sample into its place an accurate determination is made of the crossed-polarizer position in polarizer–analyzer (PA) system. In this method, the relative intensity  $\Gamma$  of transmitted light is a function of two angles  $\theta$  and  $Y$ , the azimuth angle and the deflecting angle of the analyzer from the crossed-polarizer

conditions respectively, involving the slight systematic errors  $p$ ,  $q$  and  $\delta Y$  [2,27,28].

$$\Gamma(\theta, Y, p, q) = A(\theta, p, q) + B(\theta, p, q)Y + Y^2, \quad (9)$$

$$A(\theta, p, q) = A_0 + (\gamma - 2k)\sin^2(\Delta/2) + (\gamma - 2k)\delta Y \sin \Delta + \delta Y^2 \cos^2(\Delta/2) + 4\sin^2(\Delta/2)\theta^2, \quad (10)$$

$$B(\theta, p, q) = (\gamma - 2k)\sin \Delta + 2\delta Y \cos^2(\Delta/2) + 4\sin^2(\Delta/2)\theta, \quad (11)$$

The  $A(\theta, p, q)$  and  $B(\theta, p, q)$  are acquired by the least-squares fitting of  $\Gamma$  as a function of  $\theta$ . The parameters  $p$ ,  $q$  are the parasitic ellipticities of the light emerged from polarizer and analyzer respectively. The first step in the HAUP method is to evaluate the systematic errors  $\gamma = p - q$  and  $\delta Y$ . If a specimen contain an optical nonactive phase, a characteristic  $\gamma$  value can be determined in this phase beforehand. Then the ellipticity  $k$  and  $\Delta n$  in  $\Delta$  of the optically active phases can be obtained by using this  $\gamma$  value and gyration  $G$  in calculated used equation (5).

If the specimen has no optically nonactive phase, the problem is successfully solved by using a reference crystal which is optically nonactive (for example  $\text{LiNbO}_3$ ,  $\text{LiTaO}_3$  or  $\text{CaCO}_3$ ) [29]. The determination of  $\delta Y$  can be made by using the following formula

$$\theta_0 = -\frac{1}{2}(p + q)\cot(\Delta/2) - \frac{1}{2}\delta Y. \quad (12)$$

where  $\theta_0$  is the deflecting angles between the principal axis of the indicatrix of the specimen and the observed extinction positions.

One may assume that  $p$  of the optical system will be unchanged when the reference crystal is replaced by the specimen, since the relative position of the polarizer with respect to the incident light remains unchanged. On the other hand,  $q$  may change, because the angle of incidence and the position of the emergent light from the specimen at the analyzer will be changed by this operation. In this case also  $\delta Y$  value will change as well.

This procedure was used for definition of  $g_{11}$  of (+)- and (-)-quartz [29]. From the linear relation between  $\theta_0$  and  $\cot(\Delta/2)$ , shown in Fig.3,  $(p+q)$  value was determined to be  $-1.71 \times 10^{-3}$  rad. Using  $\text{LiNbO}_3$  as reference crystal the mean value of  $p$  was calculated as  $\bar{p} = 3.13 \times 10^{-4}$  and  $\gamma = \bar{p} - q = 2.33 \times 10^{-3}$ . Also  $\delta Y = 2.29 \times 10^{-3}$  was obtained from the value  $B(0)$  at  $\Delta = 48\pi$ . The temperature dependence of  $g_{11}$  for the (+)-quartz is shown in Fig.4.

The same procedures were applied to a (-)-quartz for the (100) and (010) plates, thus

the  $g_{22}$  are in good agreement with the  $g_{11}$  of the same (-)-quartz specimen (Fig. 5).

Despite of the careful measuring which have been carried out by Kobayashi et al, it is possible to note differences between  $g_{11}$  values in (+) (Fig. 4) and (-)-quartz (Fig. 5). The  $g_{33}$  gyration component is measured rather precisely and the optical rotatory power in a quartz is used for making the etalons of the polarization plane rotation angle.

The successful determination of the optical activity for different crystals using HAUP have been reported by Meekes and Janner [30],

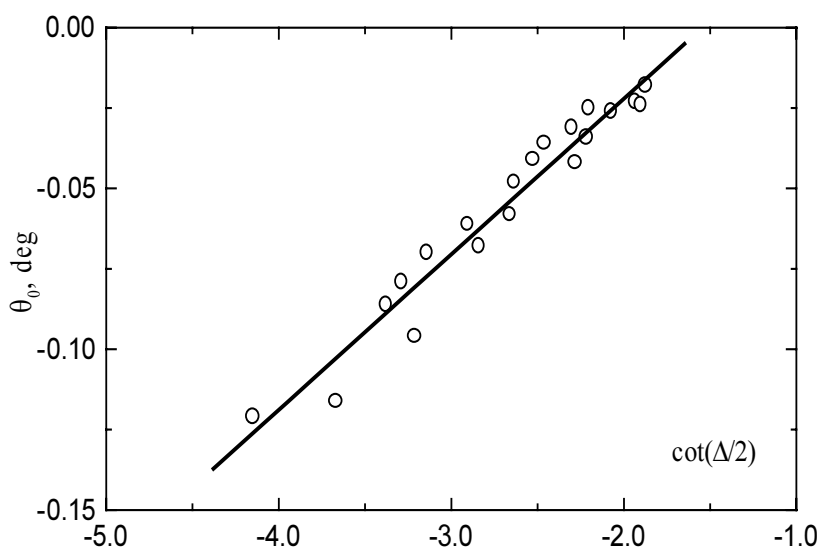


Fig. 3 Plot of  $\theta_0$  on  $\cot(\Delta/2)$  for the (100) plate of (+)-quartz [29].

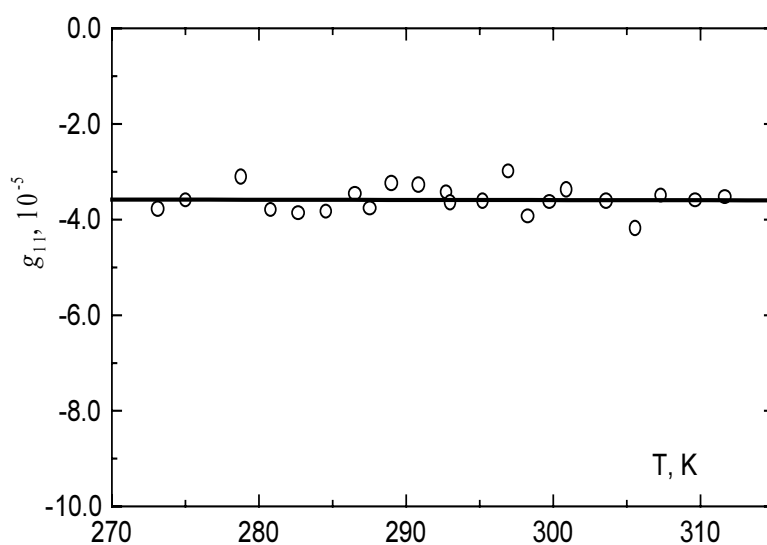


Fig. 4 Temperature dependence of  $g_{11}$  for the (100) plate of (+)-quartz [29].

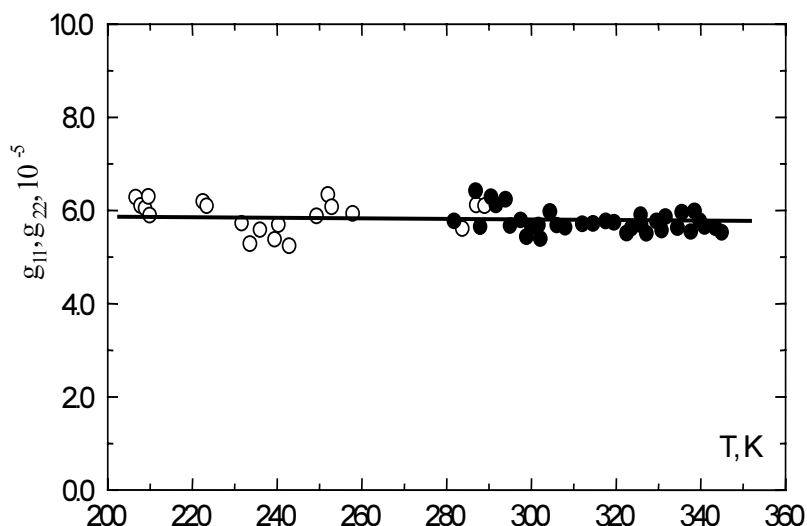


Fig. 5 Temperature dependencies of  $g_{11}$  for the (100) plate (filled circle) and  $g_{22}$  for the (010) plate (open circle) of (-)-quartz [29]

Dijkstra et al [8,31], Horinaka et al [32], Ortega et al [7], Hernandez-Rodriguez et al [33], Saito et al [11]. Moxon and Renshaw [34,35] have shown that the HAUP also provides the possibility to determine linear dichroism and circular dichroism.

#### 4. Azimuthal rotation measurements

The methods of optical activity measuring in the case of linear birefringence presence are based on the analysis of wave interference after passing the gyrotropic crystal. The method proposed by Vlokh, Shopa and Klepatsh [36,37] is based on the polarization ellipse azimuth oscillation

measuring [15] for the light beam propagating in birefringent gyrotropic crystal.

Neglecting the second-order terms for small  $\chi$ ,  $k$  and  $\theta$  relation (6) may be written as:

$$\chi = \theta \cos \Delta - k \sin \Delta. \quad (13)$$

As it follows from (13), the polarization ellipse oscillation are caused exclusively by optical activity only at  $\theta = 0$  (Fig. 6a). This condition is not easily satisfied, since  $\Delta$  being fixed, the two magnitudes  $\theta$  and  $k$  remain still unknown. On the other hand, dependence of  $\chi$  on incident light azimuth is linear, straight line slope is being determined by  $\Delta$  phase difference

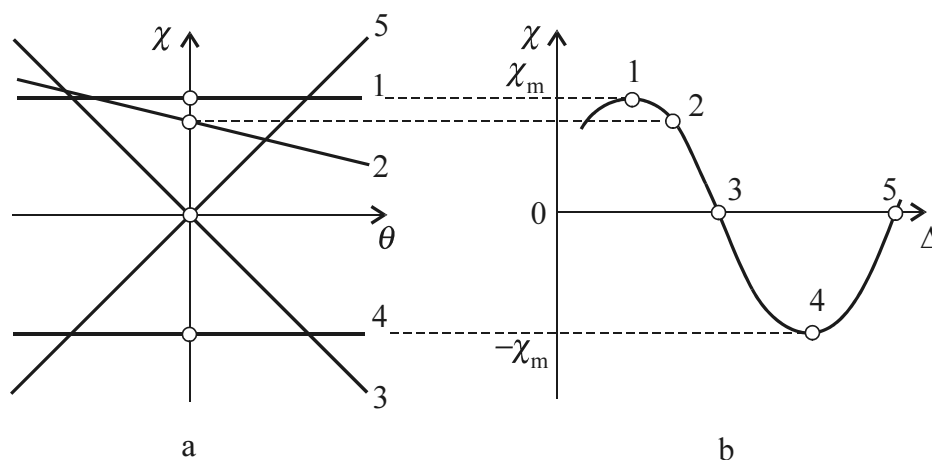


Fig. 6 The azimuth  $\chi$  dependence on the incident linear polarized light azimuth  $\theta$  (a) and on the phase difference  $\Delta$  (b)

(Fig. 6b). Thus, the  $\chi_m = \pm k$  straight lines at  $\Delta = 2\pi(m \pm 1/4)$  may be used for the  $g_{11}$  gyration tensor component determination, where  $m$  are integer numbers. Then

$$g_{11} = 2\chi_m \bar{n} \Delta n, \quad (14)$$

where  $\Delta n$  is the linear birefringence. In the case of nongyrotropic crystal all the straight lines intercept in one point.

The experimental measuring of the  $\chi$  dependencies on  $\theta$  in the  $\theta = 0$  vicinity for different  $\Delta$  changing with the temperature was the base of this technique. Electrical field being applied to the crystal, the line of the  $\chi$  on  $\theta$  dependence is shifted due to electrogyration effect while electro-optical effect is revealed in the line slope change. Thus there is possibility of simultaneous and separate determination of the electrogyration and electro-optical coefficients.

The measurements were carried out with the help of precise polarimetric apparatus containing a He-Ne laser ( $\lambda = 633$  nm), a quarter-wave plate, a polarizer, the studied crystal, the

Faraday cell, analyzer, a photo-registration system, a synchronous detector and zero-indicator. The polarizer and analyzer were equipped with angle measuring devices, the accuracy being equal to  $0.0005^\circ$ . The sample temperature was kept with 0.01 K accuracy by the special nitrogen cryostat with the polarizer and Faraday cell used as its windows.

Oscillations  $\chi(T)$ , which were used in [37] for definition of temperature dependence of the optical activity of KDP group crystals are presented in Fig. 7.

With determining of periods of oscillations, it is also possible to obtain the temperature dependencies of the linear birefringence similarly to the HAUP method. For this purpose it is necessary to measure  $\Delta n$  value and sign of quantity  $\partial \Delta n / \partial T$  for some temperature by other method (for example, by spectral method or with the Babinet compensator). The same problem exists in the Senarmont method of studying the changing of the linear birefringence.

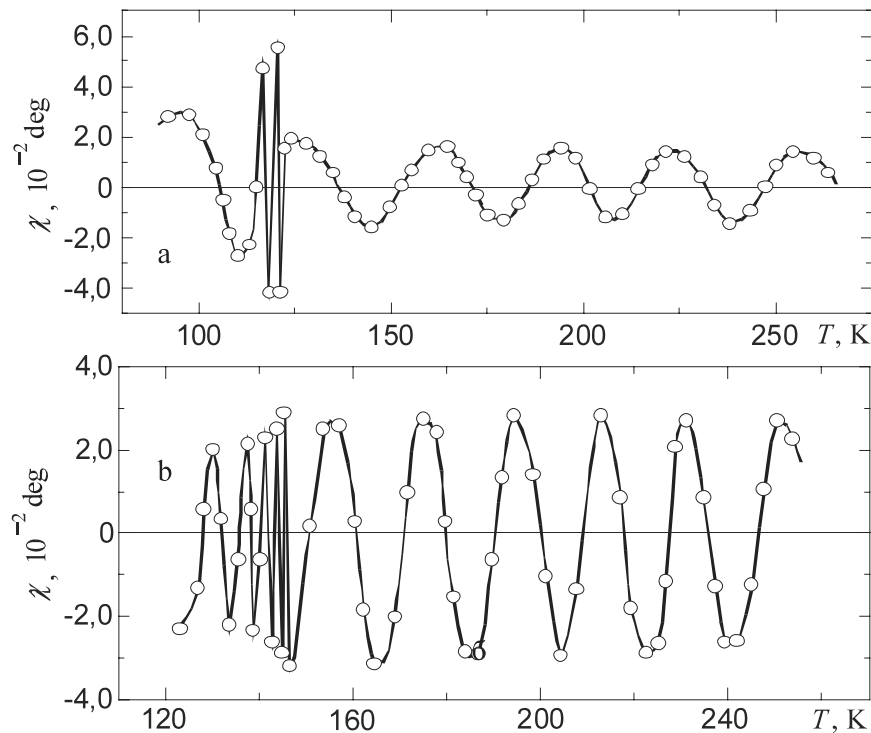


Fig. 7 The azimuth  $\chi$  temperature oscillations for KDP (a) and RDP (b) crystals [37]. Thickness  $d_x = 2,30$  mm and  $4,36$  mm respectively,  $\lambda = 633$  nm.



The results of first measuring of optical activity and electrogyration in KDP group of crystals latter were checked and confirmed by perfect HAUP-methods [38].

### 5. High accuracy PSCA null polarimeter

Proposed by Vlokh, Kushnir and Shopa [39] the method for studying of optical activity permits the measurements of polarization azimuth  $\chi$  and ellipticity  $\varepsilon$  of the polarized light emergent from a crystal sample. The measurements of  $\chi$  are performed by a “null” method in PSA optical system, and the measurements of  $\varepsilon$  in polarizer-sample-compensator-analyzer (PSCA) system, where a quarter-wave plate is used as a compensator. Besides, the procedures of coordination of polarizer, analyzer and compensator scales in polarizer-analyzer (PA) and polarizer-compensator-analyzer (PCA) system are also used.

Under the condition of small azimuths  $\theta$  of incident light the polarization azimuth  $\chi$  of the light emergent from a crystal sample may be written as

$$\chi = \theta \cos \Delta + (k - p) \sin \Delta - \delta V_{\text{PSA}}. \quad (15)$$

This relation differs from (13) by presence of the parameters  $p$  and angular systematic error of analyzer in PSA system  $\delta V_{\text{PSA}}$ . The analyzer

parameters  $q$  and  $\delta V$  depends on the conditions of propagation of light and changes its value in various optical systems, i.e.  $\delta V_{\text{PA}} \neq \delta V_{\text{PSA}}$ ,  $q_{\text{PA}} \neq q_{\text{PSA}} \neq q_{\text{PCA}}$ , etc.

Since it is difficult to measure absolute values of  $\theta$  and  $\chi$  azimuths and it is possible to register only the equality of the azimuths of the incident light and the light emerged from a sample (invariant azimuth  $\theta_0$ ) on the basis of measurements in PA system

$$\theta_0 = (k - p) \cot(\Delta/2) + (\delta\chi/2) \sin(\Delta/2). \quad (16)$$

where  $\delta\chi = \delta V_{\text{PA}} - \delta V_{\text{PSA}}$ .

The ellipticity  $\varepsilon$  passing through a crystal sample may be experimentally found from the measurements, with the use of minimum intensity method in PSCA system. The value of the characteristic ellipticity  $\varepsilon_0 = \varepsilon(\theta_0)$  [39]

$$\varepsilon_0 = 2k - p_0 + \delta\chi \cot(\Delta/2), \quad (17)$$

where  $p_0 = (3p + q_{\text{PCA}} - \delta V_{\text{PA}} - \delta V_{\text{PCA}} + 2 \delta V_{\text{PSCA}})$ . It is clear that the influence of angular parameter  $\delta V$  on  $\varepsilon_0$  value vanishes under the ideal condition of equality of  $\delta V$  values for all optical systems in which  $\chi$  and  $\varepsilon$  are measured. However in the equipment, which was used in [39], the influence of angular parameter is rather significant.

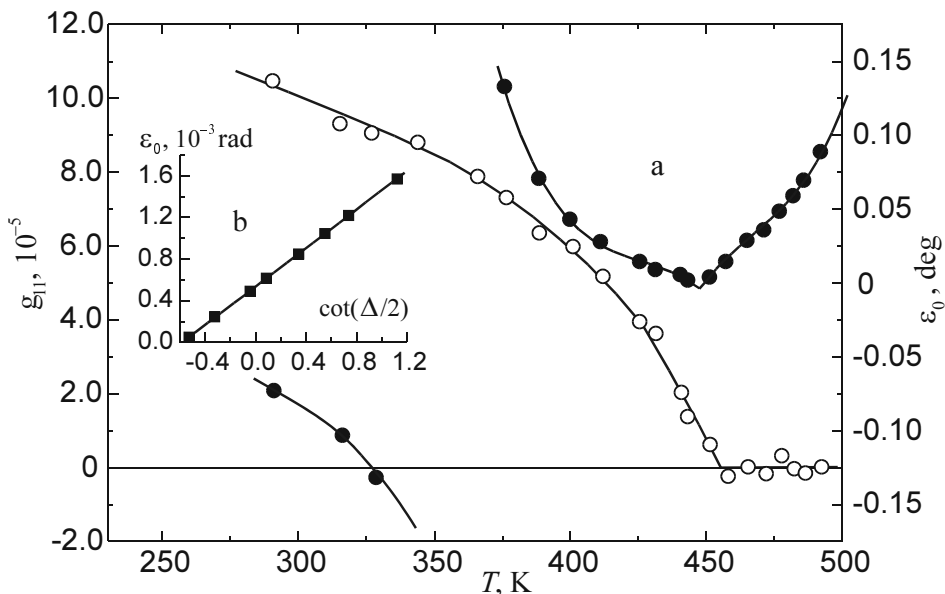


Fig. 8 Temperature dependencies of  $\varepsilon_0$  (●) and  $g_{11}$  (○) for single domain lead germanate crystal (a) and  $\varepsilon_0$  on  $\cot(\Delta/2)$  in paraelectric phase (b),  $\lambda = 633$  nm [39].

The temperature dependencies of  $\varepsilon_0$  and  $g_{11}$  for single domain lead germanate  $\text{Pb}_5\text{Ge}_3\text{O}_{11}$  are presented in Fig. 8a. Since both  $p_0$  and  $\delta\chi$  from (17) are assumed to be independent of the temperature, the dependence of  $\varepsilon_0$  on  $\cot(\Delta/2)$  in paraelectric phase, where  $k=0$  according to symmetry considerations, must be linear. The experimental data are in good agreement with these assumptions (Fig. 8b). The values  $p_0 = -5.43 \times 10^{-4}$  and  $\delta\chi = 9.10 \times 10^{-4}$  are obtained on this basis. As it could be seen, the values  $k$ ,  $p_0$  and  $\delta\chi$  are of the same order of magnitude. The divergence of  $\varepsilon_0$  at  $T_0 = 354$  K appeared only due to the temperature behaviour of the term  $\delta\chi \cot(\Delta/2)$  in (17).

In most cases no optical components are placed between the sample and polarizers. It is very important because the residual strain birefringence of the windows can produce systematic errors which make the final results completely unreliable.

## 6. Polarimetric method related to HAUP

One more measuring method of optical activity in birefringent direction [40,41] that differs from HAUP is also based on a precise measurement of relative intensity  $I$  in PSA system

$$I = (\theta - \chi)^2 + 4\theta\chi \sin^2 \frac{\Delta}{2} + 2\theta[(k+q)\sin\Delta - \delta\chi \cos\Delta] - 2\chi[(k-p) - \delta\chi] + \text{const.} \quad (18)$$

In a frame  $(\theta, \chi)$  the minimums of intensities  $I(\theta, \chi)$  the absence of a sample (PA system) are on a straight line with a slope angle  $45^\circ$  (Fig. 9). In the system PSA the minimum of intensities are also on a straight line, and the tangent of an angle of its declination is equal to  $\cos\Delta$ . Thus, the optimum scanning area of the analyzer (when a minimum is in the middle) depends on a phase difference  $\Delta$ . On a so-called HAUP-map (Fig. 9) linear dependencies  $\chi_{\text{PSA}}(\theta)$  divide the scanning area on the halves. Projections of the cuts of a surface  $I(\theta, \chi)$  by

planes  $I = \text{const}$  here are reduced and in general they have the shape of ellipses. To the centres of ellipses corresponding to the least intensity – global minimum. Optical activity and the systematic errors of a polarization system in the same way lead to the shifting of the global minimum from the center of coordinates system  $(\theta, \chi)$ .

In a HAUP procedure the similar map is represented in coordinates  $(\theta, Y)$  ( $Y = \chi - \theta$ ), the scanning area  $(\Delta\theta \times \Delta\chi)$  is square [7,8] and can contain unfavorable area for the further approximation, as well as the position of a global minimum, eccentricity and orientation of elliptical cuts on the surface  $I(\theta, \chi)$  are unknown beforehand. Therefore definition of the relevant coefficients at  $Y^2$ ,  $\theta^2$ ,  $\theta Y$ ,  $Y$  etc. and calculation of an optical anisotropy parameters ( $k$ ,  $\Delta$ ) will also be inexact. To adjust the process of measuring by HAUP -method is impossible, as well as it does not give the intermediate outcomes.

The main feature of the polarimetric method related to HAUP consists in the searching of the position of three characteristic azimuth angles of the incident light in the PSA

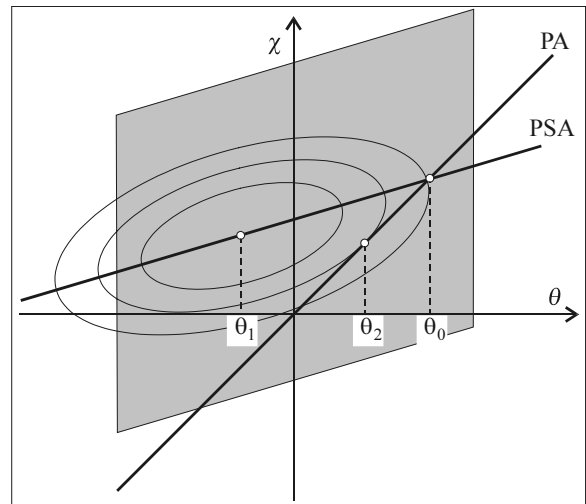


Fig. 9 The HAUP-map with positions of characteristic angles, which explains process of measurements behind a circumscribed method. The ellipses are the result of the cutting of a surface  $I(\theta, \chi)$  by planes of equal intensities. As parallelograms of the scanning area of a polarizer and analyzer in the PSA system are selected.

system, with the preceding co-ordinating of the polarizers and analyzers scales. The polarization azimuth  $\chi$  of the light emergent from a crystal is defined by the formula (15)

The intersection of linear dependencies  $\chi_{\text{PSA}}(\theta)$  and  $\chi_{\text{PA}}(\theta)$  gives the position of the so-called invariant azimuth  $\theta_0$  [39] (see formula (16)).

The value of the azimuth  $\theta_1$  for which the ellipticity of the light passed through the PSA system is equal to zero and corresponds to a global minimum of the emergent light intensity within the HAUP method is calculated by

$$\theta_1 = (k - p) \cot \Delta - (k + q) / \sin \Delta. \quad (19)$$

The third characteristic azimuth  $\theta_2$  can be interpreted as the polarizer position that corresponds to a minimum light intensity between the crossed polarizers and can be defined by (12).

It is impossible to measure the absolute values of these angles, because the start point for azimuth  $\theta$  is unknown, that's why experimentally only their differences are measured:  $\Delta\theta_{01} = \theta_0 - \theta_1$ ,  $\Delta\theta_{02} = \theta_0 - \theta_2$ ,  $\Delta\theta_{12} = \theta_1 - \theta_2$ . For them following relations:

$$\Delta\theta_{01}(1 - \cos \Delta) = (2k - \gamma) \tan(\Delta/2) - \delta\chi, \quad (20)$$

$$\Delta\theta_{02} \tan(\Delta/2) = 2k - \gamma - \delta\chi \cot(\Delta/2), \quad (21)$$

$$2\Delta\theta_{12} \cot(\Delta/2) = -2k + \gamma + \delta\chi \tan(\Delta/2) \quad (22)$$

should be satisfied. From three characteristic azimuths it is sufficiently to determine only two, or one of characteristic values  $\Delta\theta_{01}$ ,  $\Delta\theta_{02}$ ,  $\Delta\theta_{12}$ . However, experimentally characteristic azimuths are measured by independent procedures. It can be seen for example, that

$$\Delta\theta_{01}(1 + \cos \Delta) = 2\Delta\theta_{02}. \quad (23)$$

It makes enable to check out relation (23) and to control the experiment. The accuracy of the determination of  $\theta_0$ ,  $\theta_1$  and  $\theta_2$  depends on phase difference  $\Delta$ . In particular, in vicinity of  $\cos \Delta = -1$  the  $\theta_1$  is difficult to be measured, because the eccentricities of ellipses in a Fig. 9

become very small. However,  $\theta_0$  and  $\theta_2$  are determined with high precision, as well as straight lines  $\chi_{\text{PA}}(\theta)$  and  $\chi_{\text{PSA}}(\theta)$  practically intersect under straight angle. The most unfavourable from experimental point of view is a domain in which  $\cos \Delta \approx 1$ , all characteristic azimuths are measured lustily inexactly, and straight  $\chi_{\text{PA}}(\theta)$  and  $\chi_{\text{PSA}}(\theta)$  become almost parallel.

To determine the systematic error  $\gamma$  we have previously used previously the samples of the optically nonactive crystals. Basing on the experimental results for those crystals and utilizing, according to (20) and (21), the linear dependencies of  $\theta_2$  on  $\cot(\Delta/2)$  and  $\Delta\theta_{01}(1 - \cos \Delta)$  on  $\tan(\Delta/2)$ , we have found out the parasitic ellipticity  $p$ . It has to be considered as a constant, since the conditions for transmitting the laser beam through the polarizer remain invariable. After that, this value was used for determining the  $\gamma$  parameter in the following experiments with optically active crystals. To interpret the experimental results correctly, one has to know the orientation of the fast principal axis of the investigated crystals.

Another possibility for the determination of the  $\gamma$  arises from the conduction of the measurements for two orthogonal orientations of optically active crystal in polarimetric system. At the turning of the crystal on  $90^\circ$  around the optical beam -  $k \rightarrow -k$  and  $\Delta \rightarrow -\Delta$  should be replaced in (20–22). With  $\Delta\theta'_{01}$  and  $\Delta\theta''_{01}$  the characteristic for these two orientation, one can find

$$\gamma = \frac{1}{2}(\Delta\theta''_{01} + \Delta\theta'_{01}) \sin \Delta. \quad (24)$$

The latter procedure is more correct than turning the polarizers on  $90^\circ$ , because the optical conditions are practically unchanged.

Contrary to  $\gamma$ , the  $\delta\chi$  systematic error may be eliminated only by the first method, i.e. using optically nonactive crystal. However, the effect of the  $\delta\chi$  error depends essentially on the phase difference  $\Delta$ , as can be seen from (20–22). By

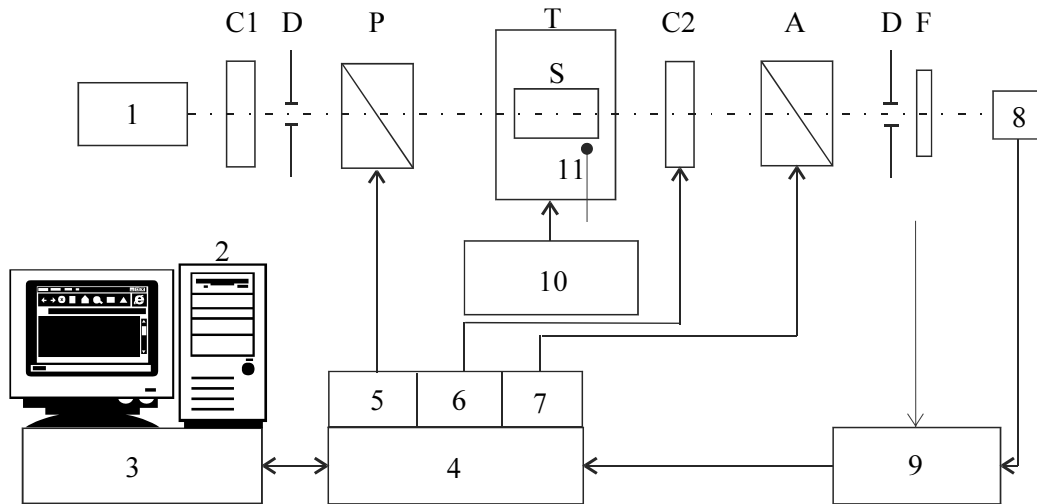


Fig. 10 Schematic diagram of the related to HAUP equipment. P - polarizer; A - analyzer; T, S - thermostat with sample; C1 - quarter-wave plate; C2 - compensator in PSCA scheme; D - diaphragm; F - filter; 1 - laser; 2 - computer; 3 - IEEE interface; 4 - interface and stepping motor controller; 5,6,7 - stepping motor; 8 - photodetector; 9 - digital voltmeter; 10 - driver of the temperature.

choosing a sample with small thickness and by satisfactory condition  $\Delta \approx (2m+1)\pi$  with  $m$  an integer, one can diminish the  $\delta\chi$  error influence, even if the temperature of the crystal is changed.

On Fig. 10 our experimental set-up is shown schematically. The specimen is placed in thermostat without optical windows. The polarizers are orientated very accurately by stepping motors. The smallest rotation angle equals  $0.0013^\circ$ . We have used a 3 mW He-Ne laser ( $\lambda = 633$  nm) as the light source. The intensity of the outgoing light is determined with the help of photodiode and digital voltmeter. The temperature reading, orientation of the polarizers and the reading of the light intensity is controlled by the computer.

Before setting the sample in its place, the crossed-polarizer position is accurately determined. At the beginning of the measurement with the crystal the  $\theta$  and  $\chi$  angles (see equation (18)) were minimized manually. Then for each polarizer position between  $-0.5^\circ$  and  $0.5^\circ$  (usually 15 points) the outgoing intensity as function of the analyzer position (30 point) is measured and minimum of the transmitted intensity is calculated.

Further we will illustrate some of the fitting procedure with measurements of optical activity on a  $x$ -cut sample of  $\text{La}_3\text{Ga}_5\text{SiO}_{14}$ .

### 6.1. Experiments with optically nonactive samples

The systematic apparatus errors may be determined by the experiments with optically nonactive samples ( $k=0$ ). The parasitic ellipticity of polarizer  $p$  may be found most exactly, since it does not vitally change its value in different polarimetric schemes. To check this affirmation two control samples were used:  $\text{LiNbO}_3$  (point group 3m, plate of 0.47mm thickness oriented along [010] direction) and  $\text{NaBi}(\text{MoO}_4)_2$  (point group 4/m, plate of 0.58 mm thickness oriented along [100] direction). All the measurements were performed in the temperature region from 287 to 322 K, using polarimetric PSA system to find the characteristic angles. From the dependencies of  $\Delta\theta_0 \sin\Delta$  on  $\tan(\Delta/2)$  (Fig. 11.) and  $\theta_2$  on  $\cot(\Delta/2)$  one can determine  $\gamma = 9.74 \times 10^{-4}$  and  $p + q = 1.50 \times 10^{-4}$ . Thus, we have  $p = 5.62 \times 10^{-4}$  and  $q = -4.12 \times 10^{-4}$ . In the same manner,  $p = 4.85 \times 10^{-4}$  and  $q = 1.14 \times 10^{-4}$  for  $\text{NaBi}(\text{MoO}_4)_2$  is obtained. As it is seen from

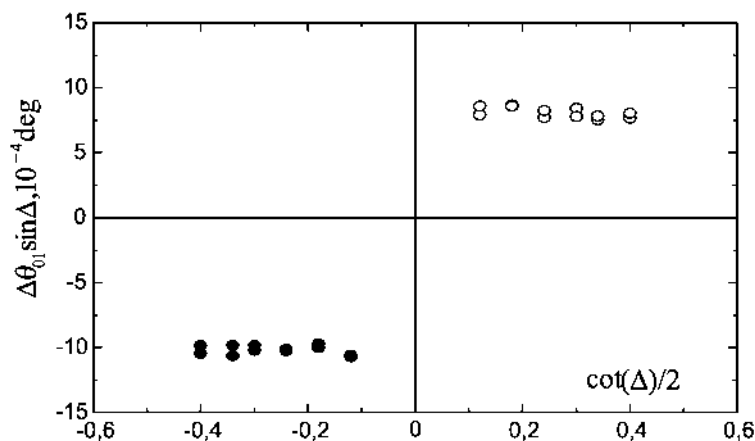


Fig. 11. Relation between  $\Delta\theta_{01} \sin \Delta$  and  $\cot(\Delta/2)$  for  $\text{La}_3\text{Ga}_5\text{SiO}_{14}$  before ( $\circ$ ) and after turning of the sample by  $90^\circ$  ( $\bullet$ ) [40].

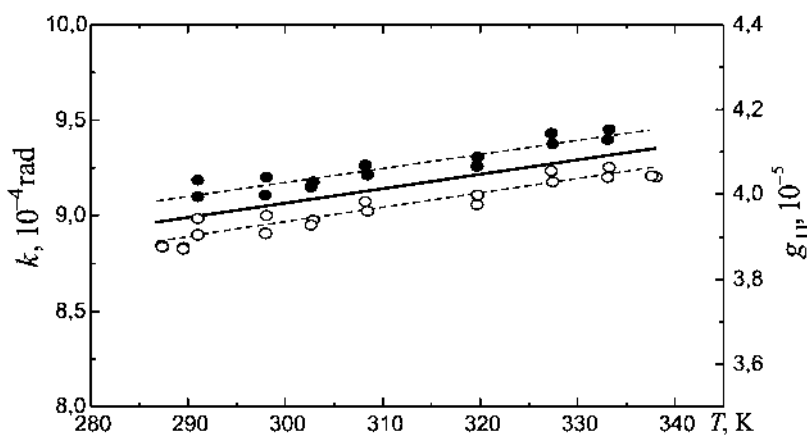


Fig. 12. Temperature dependencies of  $k$  and  $g_{11}$  for the (100) plate of  $\text{La}_3\text{Ga}_5\text{SiO}_{14}$  obtained by using the procedure of the turning of the sample by  $90^\circ$  ( $\bullet$ ) and the additional procedure with optically inactive sample ( $\circ$ ). The dashed lines are least square fits for the two mentioned cases and the solid ones represent the averaged results [40].

these results,  $p$  varies only slightly. Its average value can be used in further experimental calculations with another samples. It is significant to keep unchanged the optical conditions concerning the polarizer.

The value of  $\delta\chi$  was determined as the intercept of the dependence (20) with the ordinate axis. The averaged value of this systematic error for two control samples is  $\overline{\delta\chi} = 3.32 \times 10^{-6}$ . Then, according to formula (20) and using the linear dependence of  $\theta_2$  on  $\cot(\Delta/2)$  measured for  $\text{La}_3\text{Ga}_5\text{SiO}_{14}$  and the values  $p$  and  $\delta\chi$ , we obtain

the temperature dependence of the eigenwave ellipticity  $k$  (Fig. 13).

## 6.2. Sample rotation by $90^\circ$

Despite of simplicity of this procedure, its realization demands diligent preparation. It is believed that, under the turning of the crystal by  $90^\circ$  around the laser beam axis, the systematic errors  $p$ ,  $q$  and  $\delta\chi$  remain unchangeable. It is obvious that, in order to fulfil this condition, the investigated sample must be ideally plane parallel, the region where the laser beam passed through the crystal should not be changed, and the turning

angle must be very close to  $90^\circ$ . When these demands are satisfied, then the slopes of the linear dependencies of  $\theta'_2$  on  $\cot(\Delta/2)$  are measured before and after turning of the crystal and they are the same in the absolute value but opposite in sign. Furthermore, we used the same set of temperature points for these two orientations. It made possible to determine separately the difference  $\Delta\theta'_{01} - \Delta\theta''_{01}$  at each temperature, and the average  $\gamma$  value only at the final stage. In this case we were to obtain -  $\gamma = 1.07 \times 10^{-4}$ .

The temperature dependence of  $g_{11} = k/(2n\Delta n)$  derived by this method is in good agreement with the results obtained using the control samples (Fig. 12). Thus, behind functionalities the offered method does not differ from HAUP. At the same time it is more simple in the instrumentation and also gives intermediate control outcomes, which allow to track the measuring process.

## 7. Tilter polarimeter

Technique of high accuracy polarimetry is quite popular. Different laboratories use it in various versions, particularly in the version of spectropolarimetry. For example, WS-HAUP equipment (wavelength-scanning high-accuracy

universal polarimeter) is built in Oxford [35,42]. This technique is quite slow (a single scan takes about two days). Some crystals can change their properties during such a long measuring process. That's why a search of speed methods in polarimetry is actual. Recently, the 'tilter' method has been developed by Kaminsky and Glazer [43,44]. This method is also based on the HAUP technique, but here a plane-parallel cut sample plate is tilted around an axis perpendicular to the incident light wave. Furthermore, a fixed wavelength is used. The new system allows to use a laser and fast light-intensity measurements, whilst the retardation is changed by the tilting. In this way the time for a complete scan can be reduced, typically to 5 min. [5].

A schematic diagram of the tilting apparatus is shown in Fig. 13. In the tilting system the intensity  $I_0$  of the incident linear-polarized light is approximately related to the intensity  $I$  resulting from light interaction with the following sequence: polarizer (at angle  $Y + 90^\circ$ ), sample (with angle of extinction  $\theta$ ), and analyzer (at angle  $\Omega$ ). The angles are measured with respect to the tilt axis, which is perpendicular to the wave vector.

$$\frac{I}{I_0} \approx (\varphi + \Omega)^2 + (\varepsilon + q)^2 \quad (25)$$

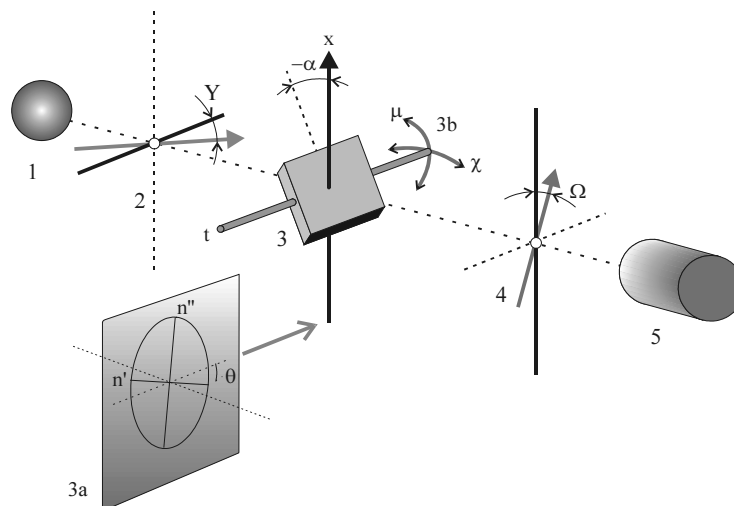


Fig. 13. The set-up of the tilter-system. (1) Laser diode, (2) polarizer, (3) tilt axis, (3a) shape of the optical-indicatrix section, (4) analyzer system: quarter-wave plate, Pockels modulator (NH<sub>4</sub>H<sub>2</sub>PO<sub>4</sub> single crystal cut on (001) with transparent electrodes) analyzer, (5) detector [4,9].

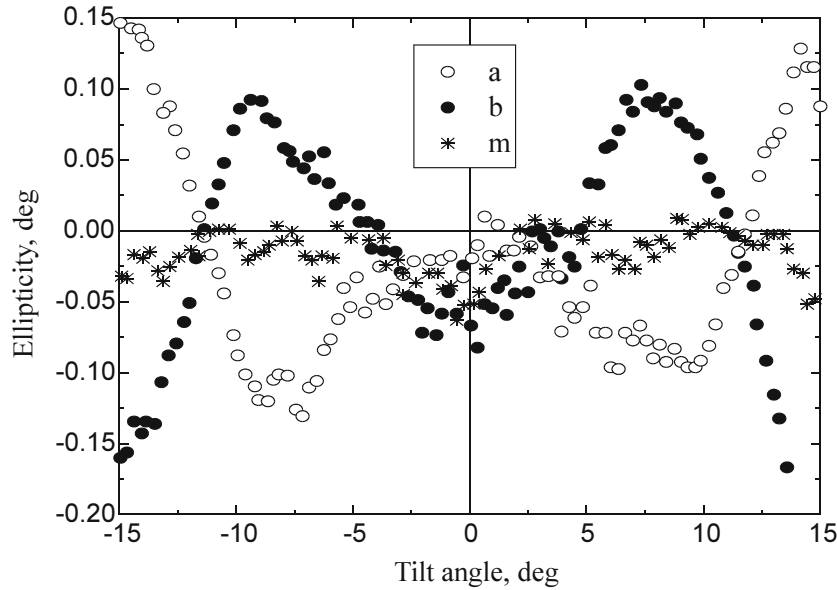


Fig. 14. Tilt scans in KDP, cut on (001) with **a** tilt towards the crystallographic axis *a*; **b**, tilt towards *b*; **m**, tilt towards the meridian between *a* and *b*,  $\lambda = 680$  nm [5].

where

$$\varphi \approx \varphi_0 \frac{\sin \Delta}{\Delta} + Y \cos \Delta + 2\theta \sin^2 \frac{\Delta}{2} + q \sin \Delta,$$

$$\varepsilon \approx \frac{2\varphi_0}{\Delta} \sin^2 \frac{\Delta}{2} + (Y - \theta) \sin \Delta + 2\theta - p \cos \Delta,$$

$\varphi$  is the azimuthal angle of rotation with respect to the initial light polarization,  $\varepsilon$  is the ellipticity of the sample,  $\varphi_0$  is the optical rotation (plate thickness multiplied by rotatory power). Equation (25) is derived on the assumption that all angular quantities, with the exception of  $\varphi_0$ , are small.

Last equation can be rewritten in the form of a polynomial expression, as shown by Kaminsky and Glazer [9]:

$$\frac{I}{I_0} = a_0 + a_1 \Omega + a_2 Y + a_3 \Omega Y + \Omega^2 + Y^2 \quad (26)$$

$$\text{where } a_1 \approx 2 \left( \frac{\varphi_0}{\Delta} + p \right) \sin \Delta + 2\theta(1 - \cos \Delta),$$

$$a_2 \approx 2 \left( \frac{\varphi_0}{\Delta} + p \right) \sin \Delta - 2\theta(1 - \cos \Delta),$$

$$a_3 \approx 2 \cos \Delta.$$

In the tilting method the resulting intensity  $I$  is measured for successive  $\beta$  angles as the function of  $Y$  and  $\Omega$ , and then equation (26), which defines the surface in three-dimensional

space ( $I$ ,  $Y$  and  $\Omega$ ), is fitted to the experimental points (typically for each tilt angle  $\beta$  about one hundred experimental points are collected within the ranges  $-0.7^\circ < Y < 0.7^\circ$  and  $-0.7^\circ < \Omega < 0.7^\circ$ ).

It is useful to define functions  $y_1(\beta)$ ,  $y_2(\beta)$  and  $y_3(\beta)$  in such a way that  $y_1(\beta)$  consists of the gyration-related signal generated from  $a_1(\beta) + a_2(\beta)$ , i.e. it contains  $(\varphi(\beta)\Delta^{-1} + 2p + \gamma)\sin \Delta$ .  $y_2(\beta)$  related to  $a_1(\beta) - a_2(\beta)$  and depends on  $\theta(\beta)[1 - \cos \Delta(\beta) + \gamma]$ , whereas  $y_3(\beta)$  follows the  $\cos \Delta(\beta)$  distribution.  $\gamma$  contains the difference between  $q$  and  $p$  as well as other parasitic ellipticities are caused by the reflection and depolarization of the sample. Figure 3 shows schematically a typical analysis of the functions  $y_1(\beta)$ ,  $y_2(\beta)$  and  $y_3(\beta)$  using as input parameters: retardation of the crystal cut  $\Gamma = \Delta nd$ . In the first step the numerical inversion of  $y_3(\beta)$  into  $\Delta(\beta)$  is carried out according to the special procedure.

Assuming that the indicatrix is roughly oriented with one principal direction parallel to the initial polarization, the principal refractive indices  $n_1$  and  $n_2$  in relation to  $n_E$  are calculated by a linear fitting procedure, where  $\beta' = (\beta - \beta_0)$

and  $\beta_0$  is not constrained. The further nonlinear refinement of  $n_1$ ,  $n_2$ , and  $\beta_0$  is carried out using the experimental  $y_3(\beta)$ . Subsequent analysis of the function  $y_2(\beta)$  is able to determine the orientation of the indicatrix and parasitic effects which are related to the adjustment of the analyzer and depolarizing effects of the crystal. Finally, the analysis of  $y_1(\beta)$  allows to eliminate the polarizer ellipticity  $p$  and sum the parasitic effects ( $\gamma$  and  $\delta Y$ , which is an error mainly caused by the offset in  $Y$  of the polarizer). The output of the program contains the refined principal refractive indices in relation to  $n_E$ , indicatrix orientation ( $\beta_0$ ,  $\chi$ ,  $\mu$ ) rotatory power along the plate normal  $\mathbf{n}$ , rotatory power perpendicular to  $\mathbf{n}$  and the tilt axis, and the ellipticity  $y_1^{\text{tiltered}} = \varphi_0(\beta)\Delta^{-1}(\beta)\sin\Delta(\beta)$ .

According to the assertions of the authors, this method is independent of the parasitic ellipticity of the analyzer system as well as of the parasitic ellipticity of the sample, whatever its origin is.

At the beginning of each measurement with the tilter system, the  $\chi$  and  $\mu$  angles (see equation (26) and Fig. 13) were minimized manually by making a test scan. After each complete tilt scan the sample was rotated through  $90^\circ$  about the direction of the incident light and the whole measurement procedure was repeated. In order to improve the elimination of parasitic ellipticities of the set-up [2,34] the average result for both orientations were taken for further calculations.

The advantage of the tilter technique over HAUP and WS-HAUP methods is its speed, resulting from a much more higher initial intensity  $I_0$  by using a laser. In WS-HAUP a monochromator is used in combination with a white-light source [35]. The parasitic ellipticities are separated out in repeating the measurement with the sample rotated by  $90^\circ$ , which transforms  $\Delta$  into  $-\Delta$ . The average scan calculated from the first and the repeated wavelength scan

is independent of the parasitic contributions. However, the  $\delta Y$  error is not completely eliminated with method (b) when the primary adjustment of the polarizer is not perfect.

As an example of a tensor determination with the ‘tilter’, the spectra of  $\varphi(\Delta)\sin(\Delta)/\Delta$  against tilt angle  $\beta$  for different crystal sections in  $\text{KH}_2\text{PO}_4$ , are shown in Fig.14. The character of oscillations confirms the fact known in a crystalloptics, that gyration components  $g_{11}$  and  $g_{22}$  possess the opposite signs.

Despite the appeal of the mentioned method from a point of view of its speed qualities, nevertheless it is possible to make some notes. The optical scheme presented on Fig. 13 contains additional optical elements with optical windows. According to [34] it could lead to the growth of systematic errors. The nonorthogonal incidence of a light requires the accounting of the additional parameters.

## Conclusion

In the present review paper not all polarimetric devices are described. The attention is payed to the image polarimetry, which recently become rather popular. However high accuracy polarimetry during last years was useful at studying of the optical properties of dielectrics and ferroelectrics. Some results for example concerning incommensurate phases, till now remain debatable. At the same time properties of the ferroelectric crystals, obtained on the basis of the measuring of temperature behaviour of an optical activity are interesting and useful for the understanding of phase transitions mechanism.

**Acknowledgements.** The author is very grateful to Professor O. Vlokh for the stationary sufficient support and interest to the present investigations. Also the author would like to thank Dr. N. Klepatsh, Dr. I. Berezhnyi, Dr. O. Kushnir and Dr. M. Kravtchuk for the essential contribution in methodical guidelines and hardware.



## References

1. Azzam R.M.A. and Bashara N.M. Ellipsometry and polarized light. Ch.2. North-Holland Physics Publishing. Amsterdam (1988).
2. Kobayashi J. Phase Transition. **36** (1991) p.95–128.
3. Condens. Matter News 2(4) (1993) p.19.
4. Vlokh O.G. Phenomena of spatial dispersion in parametrical crystal optic L'viv (1984) (in Russian).
5. Kaminsky W. J.Rep.Prog.Phys **63** (2000) p.1575–1640.
6. Konstantinova A.F., Grechushnikov B.V., Bokut' B.V. and Valjashko E.E. Optical properties of crystals "Nauka i Tekhnika" Minsk (1995) (in Russian).
7. Ortega J., Etxebarria J., Zubillaga J., Brezczewski T., and Tello J.Phys.Rew.B. **45** (1992) p.5155–5162.
8. Dijkstra E. and Janner A. Ferroelectrics **105** (1990) p.113.
9. Mucha D., Stadnicka K., Kaminsky W., Glazer A.M. J.Phys: Condens. Matter **9** (1997) p.10829–10842.
10. Konstantinova A. F., Evdischenko E.A. Proceedings SPIE **3094** (1997) p.159–168.
11. Saito K., Asahi T., Takahashi N., Higano M., Kamiya I., Sato Y., Okubo K. and Kobayashi J. Ferroelectrics **152** (1994) p.231–236.
12. Nye J.F. Physical properties of crystals. Oxford University Press, Oxford (1985).
13. Szivessy G. and Münster C. Ann.Phys. **20** (1934) p.703–726.
14. Bruhat G. and Grivet P. J.Physique Radium **6** (1935) p.12–26.
15. Konstantinova A.F., Ivanov N.R. and Grechushnikov B.N. Crystallography **14** (1969) p.283–392 (in Russian).
16. Zheludev I.S. Crystallography **9** (1964) p.501–505 (in Russian).
17. Vlokh O.G. Ukr.J. of Phys. **15** (1970) p.758–762 (in Russian).
18. Vlokh O.G., Klymiv I.M., Kobilyansky V.B. Ukr.J. of Phys. **18** (1973) p.2055–2058 (in Russian).
19. Vlokh O.G., Kobilyansky V.B. Ukr.J. of Phys. **19** (1974) p.1129–1135 (in Russian).
20. Ivanov N.R., Konstantinova A.F. Crystallography **15** (1970) p.416 (in Russian).
21. Ivanov N.R., Chikhladze O.A. Crystallography **21** (1976) p.125–132 (in Russian).
22. Kaminckii A.A., Mill B.V., Khodzhabayyan G.G., Konstantinova A.F., Okorochkov A.I. and Silvestrova I.M. Phys. stat. sol.(a), **80** (1983) p.387.
23. Vlokh O.G., Lazko L.A., Zheludev I.S. Crystallography **20** (1975) p.1056 – 1058 (in Russian).
24. Vlokh O.G., Zaryk A.V. Ukr. J. of Phys. **26** (1981) p. 1087–1090 (in Russian).
25. Vlokh O.G. Lett. J. Exp. and Theor. Phys. **13** (1971) p.118–121 (in Russian).
26. Anderson W.J., Phil Won Yu and Park Y.S. Opt. Commun. **11** (1974) p.392–395.
27. Kobayashi J. and Uesu Y. J. Appl. Cryst. **16** (1983) p.204–211.
28. Kobayashi J., Uesu Y. and Takahashi H. J. Appl. Crystallogr. **16** (1983) p.212–219.
29. Kobayashi J., Uesu Y. Takahashi H. and Glazer A.M. J. Appl. Crystallogr. **21** (1988) p.479–484.
30. Meekes H. and Janner A. Phys.Rew.B **38** (1988) p.8075.
31. Dijkstra E. Meekes H. and Kremers M. J. Phys D: Appl. Phys. **24** (1991) p.1861.
32. Horinaka H., Tomii K., Sonomura N. and Miyauchi T. Japan J.Phys. **24** (1985) p.755.
33. Hernandez-Rodriguez C., Gomez-Garrido P. and Veintemillas S. J.Appl.Cryst. **33** (2000) p.938–946.
34. Moxon J.R.L., Renshaw A.R. J. Phys: Condens. Matter **2** (1990) p.6807–6836.
35. Moxon, J.R.L., Renshaw A.R. and Tebbutt I.J. J.Phys. **D24** (1991) p.1187–1192.
36. Vlokh O.G., Klepatch N.I. and Shopa Y.I. Ferroelectrics **69** (1986) p.267–274.

37. Vlokh O.G., Klepatch N.I. and Shopa Y.I. Crystallography **31** (1986) p. 195–197 (in Russian).
38. Kobayashi J., Asahi T. and Takahashi S. Ferroelectrics **75** (1987) p.139–152.
39. Vlokh O.G., Kushnir O.S. and Shopa Y.I. Acta Physica Polonica A **81** (1992) 571–578.
40. Shopa Y.I., Kravchuk M.O. Phys. stat. sol.(a), **158** (1996) p.275–280.
41. Shopa Y.I., Kravchuk M.O. and Vlokh O.G. Proceedings SPIE **2648** (1995) p.674–679.
42. Lingard R.J. and Renshaw A.R. J.Appl.Cryst. **27** (1994) 647.
43. Kaminsky W. and Glazer A.M. Ferroelectrics **183** (1996) p.133–141.
44. Glazer A.M. and Kaminsky W. Acta Cryst. **A52** (1996) 39.